Structural Trends in Silicon Atranes

Michael W. Schmidt, Theresa L. Windus,† and Mark S. Gordon*

Contribution from the Department of Chemistry, Iowa State University, Ames, Iowa 50011

Received June 14, 1994®

Abstract: Ab initio calculations with full geometry optimization are performed on a wide range of silicon atranes, $RSi[-Y(CH_2)_2-]_3N$, where R = H, F, OH, NH_2, CH_3, Cl, SH, PH_2, SiH_3, and Y = O, NH, NCH_3, CH_2, using the 6-31G(d) or larger basis sets. The results are used to show trends in the dative SiN bond as a function of axial R and equatorial Y substitution. The SiN bond is shown to be quite weak, making the atrane geometries very sensitive to medium effects, as shown by model solvation computations. The nature of the SiN bonding is best described as dative, as shown by localized orbitals.

Introduction

Pentacoordinated silicon compounds have attracted a great deal of interest in recent decades. One well studied class of such molecules are the silatranes, Y=O, which contain an intramolecular SiN bond:

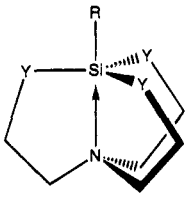

Since they were first prepared in 1961,[1] the silatranes (Y = O) have been extensively investigated, as reported in several hundred papers from the research groups of Voronkov, Corriu, Lukevits, Hencsei, and others. Numerous review articles are available,[2−7] including two compendia of the available structural data.[8,9] The silatrane structure consists of a distorted trigonal bipyramid at Si, with nearly equatorial atoms Y. The axial N is pyramidalized so that its lone pair points at Si. While most chemists have been interested in silatranes because of this geometry and its short SiN bond distance, silatranes are also of interest because of their wide range of biological activities,[10,11] which include stimulation of hair growth[10] and increased winter wheat yields.[12]

Most silatrane X-ray structures have transannular SiN bond distances in the range 2.05−2.20 Å.[8,9] Because this is considerably shorter than the sum of the van der Waals radii, 3.5 Å, silatranes are generally considered to possess a weak SiN bond, although this bond is certainly longer than the typical single SiN bond distance of 1.7−1.8 Å. The general consensus is that more electronegative groups R yield shorter SiN bonds, although the shortest known bond occurs for R = Cl (2.02 Å) instead of R = F (2.04 Å). Obviously, the extent of the SiN bonding as a function of the group R is of great interest. Although the structures of over 70 silatranes are now known,[8,9] the atom in R that is directly connected to Si is limited to H, halogen,[13] C (aryl or alkyl), and O. NMR shifts are found to correlate well with the transannular bond distance,[8,9,14] and one of the isotropic nitrogen shifts "appears to be a direct measure of the transannular interaction".[15] Ionization potentials of three silatranes[16] suggest a SiN bond strength in the range 13−22 kcal/mol.

It is certainly true that this SiN interaction is weak, and in fact this is apparent in the two available gas phase structures, for R = CH_3[17] and R = F.[18] Both of these silatranes possess gas phase structures whose SiN bond is 0.28 Å longer than that in the solid state. At the least this indicates the SiN bond is very deformable and thus weak if crystal forces can produce such a large change in geometry, and at the extreme "the dative bond which exists in the solid state for methylsilatrane is not evident in the gas phase".[17] Solution phase NMR and IR data[19] imply bond distances intermediate to the solid state and the gas phase. For example, the SiN bond in methylsilatrane is approximately 2.20−2.30 Å in various solvents, compared to 2.175 and 2.45 ± 0.05 Å in the solid and gaseous state, respectively.

The first azasilatranes (in which Y = NH) were reported in 1977,[20] for R = H, alkyl, and aryl. The chemistry of these molecules has been explored by the groups of Lukevits[20−22] and Verkade,[23−30] sometimes for Y = NCH_3 or with even

† Present address: Department of Chemistry, 2145 Sheridan Road, Northwestern University, Evanston, IL 60208-3113.

® Abstract published in *Advance ACS Abstracts*, July 1, 1995.

(1) Frye, C. L.; Vogel, G. E.; Hall, J. A. *J. Am. Chem. Soc.* **1961**, *83*, 996−997.
(2) Voronkov, M. G. *Pure Appl. Chem.* **1966**, *13*, 35−59.
(3) Voronkov, M. G.; Dyakov, V. M.; Kirpichenko, S. V. *J. Organomet. Chem.* **1982**, *233*, 1−147.
(4) Tandura, S. N.; Voronkov, M. G.; Alekseev, N. V. *Top. Curr. Chem.* **1986**, *131*, 99−189.
(5) Lukevits, E.; Pudova, O.; Sturkovich, R. *Molecular Structure of Organosilicon Compounds*; Ellis Horwood: Chichester, 1989.
(6) Corriu, R. J. P. *J. Organomet. Chem.* **1990**, *400*, 81−106.
(7) Chuit, C.; Corriu, R. J. P.; Reye, C.; Young, J. C. *Chem. Rev.* **1993**, *93*, 1371−1448.
(8) Greenberg, A.; Wu, G. *Struct. Chem.* **1990**, *1*, 79−85.
(9) Hencsei, P. *Struct. Chem.* **1991**, *2*, 21−26.
(10) Voronkov, M. G. *Top. Curr. Chem.* **1979**, *84*, 77−135.
(11) Some more recent references may be found in ref 42.
(12) Bihatsi, L.; Hencsei, P.; Kotai, L.; Ripka, G. *Novenyvedelem (Budapest)* **1992**, *28*, 180−184. (*Chem. Abstr.* 117:207034u).
(13) Voronkov, M. G.; Baryshok, V. P.; Petukhov, L. P.; Rahklin, R. G.; Pestunovich, V. A. *J. Organomet. Chem.* **1988**, *358*, 39−55.
(14) Kupche, E. L.; Lukevits, E. *Chem. Heterocyclic Compounds* (English Translation) **1989**, *25*, 586−588.
(15) Iwamiya, J. H.; Maciel, G. E. *J. Am. Chem. Soc.* **1993**, *115*, 6835−6842.
(16) Brodskaya, E. I.; Voronkov, M. G. *Bull. Acad. Sci. USSR, Chem. Sci.* (English Translation) **1986**, 1546.
(17) Shen, Q.; Hilderbrandt, R. L. *J. Mol. Struct.* **1980**, *64*, 257−262.
(18) Forgacs, G.; Kolonits, M.; Hargittai, I. *Struct. Chem.* **1990**, *1*, 245−250.
(19) Pestunovich, V. A.; Shterenberg, B. Z.; Lippma, E. T.; Myagi, M. Ya.; Alla, M. A.; Tandura, S. N.; Baryshok, V. P.; Petukhov, L. P.; Voronkov, M. G. *Doklady Phys. Chem. (English Translation)* **1981**, *258*, 587−590.
(20) Lukevits, E.; Zekhan, G. I.; Solomennikova, I. I.; Liepin'sh, E. E.; Yankevska, I. S.; Mazheika, I. B. *J. Gen. Chem. USSR (English Translation)* **1977**, *47*, 98−101.

0002-7863/95/1517-7480$09.00/0

bulkier groups such as $Si(CH_3)_3$ on the equatorial nitrogens. Very bulky groups are found to destroy the transannular SiN bond.[24] The available X-ray structures show SiN bond distances virtually identical to those in the analogous silatrane, but other data such as NMR "are consistent with the notion that a stronger SiN bond exists than in silatranes".[21] The range of R groups which have been explored for the azasilatranes is somewhat broader, consisting of H, alkyl, aryl, halogen, $N(CH_3)_2$, N_3, −NCS, −SCN, and OC_2H_5.

By analogy with the name azasilatranes, we denote the compounds with Y = CH_2 as carbasilatranes.[9] The first two members of this family, R = CH_3 and Cl, were reported in 1985.[31] Bis-carbasilatrane ether's X-ray structure[32] has a linear SiOSi angle with a long SiN distance, 2.477 Å. Some NMR experiments[33] on chlorocarbasilatrane imply SiN bond stretch isomerization, but this may be due to impurities as is the case for similar carbastannatranes.[34] In the 1970s two atranes with one Y = CH_2 and the other two Y = O were reported. Methylmonocarbasilatrane, R = CH_3[35] has a shorter axial than equatorial SiC bond, 1.877 vs 1.898 Å! On the other hand, methoxymonocarbasilatrane, R = OCH_3[36] has the axial SiO longer than equatorial, 1.672 vs 1.656 Å, as expected. Because of their asymmetry, the trigonal bipyramid in monocarbasilatranes is more distorted than usual. Perhaps most significantly, the SiN bond distance is longer than in the analogous silatrane: 2.336 vs 2.175 Å for R = CH_3 and 2.223 vs 2.11[15] Å for R = OCH_3.

The present paper extends the range of available silatrane geometries by *ab initio* geometry optimization. Silatranes (Y = O), azasilatranes (Y = NH and Y = NCH_3), and carbasilatranes (Y = CH_2) are investigated. The range of substituents R considered is H, CH_3, NH_2, OH, F, SiH_3, PH_2, SH, and Cl and is considerably broader than the range of available experimental compounds. Trends in SiN bonding as a function of Y and R are presented, and the nature of this bond is discussed. This broad investigation at a reliable level of electronic structure theory was feasible only because of the development of parallel electronic structure codes and the availability of parallel computers.

Most previous theoretical work on silatranes has been limited to semiempirical methods due to the large size of the molecules. All prior work appears to be limited to the silatranes. The first calculations[37] used CNDO/2 with *spd* basis sets, as the most popular bonding model of the time invoked sp^3d hybridization. Experimental geometries were used to calculate bond orders in phenylsilatrane by the CNDO/2 method.[38] Because a three-center bonding model had come into vogue, a 1987 CNDO/2 calculation[39] used *sp* as well as *spd* basis sets to estimate the bond orders in methylsilatrane. An important paper in 1987[40] studied the effect of solvent on the SiN bond potential in methyl- and fluorosilatrane, using MINDO/3 with an Onsager reaction field model. The presence of solvent was found to decrease the SiN bond length, in agreement with experiment. MNDO calculations[41] on methylsilatrane found a smaller bond order than for covalent SiN bonds.

The first *ab initio* calculation[42] on fluorosilatrane appeared in 1991, using a 3-21G* basis and geometries modeled after experimental solid and gas phase structures. A paper in the same year from our group[43] used *ab initio* wave functions at AM1 optimized geometries for hydroxysilatrane and found that compression of the SiN bond from the computed to the experimental value required just 6 kcal/mol. Electron density analysis confirmed the presence of a Si−N bond, even at the long gas phase structure. Finally, a series of AM1 and PM3 semiempirical results for fluoro-,[44a] methyl-,[44b] and chlorosilatrane[44c] appeared recently. These papers find two distinct minima, an *endo* silatrane and an *exo* structure, in which the SiN bond is absent. There is a slight energetic preference for the *endo* forms, but a very flat potential surface is obtained throughout the range of SiN distances considered, 2.00−3.40 Å. While this manuscript was being reviewed, the first published *ab initio* geometry optimization of fluorosilatrane appeared,[45] casting doubt on the semiempirical *exo* structures.

The consensus from all of these papers is that the SiN bond is present but weak, particularly in those papers which present a SiN potential curve. However, very little *ab initio* data are available, so the structures of 32 silatranes are presented here.

Although they do not involve silatranes, papers from our group on neutral[46] and ionic[47] five coordinate silicon species are related to the present work. Although NH_3 is found to complex to $RSiY_3$, forming $RSiY_3NH_3$, the SiN bond is weak and the most stable complex results when the other axial group is very electronegative, e.g., R = F, or if it bonds less strongly to Si, e.g., R = Cl. Finally, the present paper on silatranes and related molecules parallels a companion paper[48] on phosphatranes and azaphosphatranes.

(21) Kupce, E.; Liepins, E.; Lapsina, A.; Zelcans, G.; Lukevits, E. *J. Organomet. Chem.* **1987**, *333*, 1−7.
(22) Macharashvili, A. A.; Shklover, V. E.; Struchkov, Yu. T.; Lapsina, A.; Zelcans, G.; Lukevits, E. *J. Organomet. Chem.* **1988**, *349*, 23−27.
(23) Gudat, D.; Verkade, J. G. Organometallics **1989**, *8*, 2772−2279.
(24) Gudat, D.; Daniels, L. M.; Verkade, J. G. *J. Am. Chem. Soc.* **1989**, *111*, 8520−8522.
(25) Gudat, D.; Daniels, L. M.; Verkade, J. G. *Organometallics* **1990**, *9*, 1464−1470.
(26) Gudat, D.; Verkade, J. G. *Organometallics* **1990**, *9*, 2172−2175.
(27) Woning, J.; Daniels, L. M.; Verkade, J. G. *J. Am. Chem. Soc.* **1990**, *112*, 4601−4602.
(28) Woning, J.; Verkade, J. G. *Organometallics* **1991**, *10*, 2259−2266.
(29) Woning, J.; Verkade, J. G. *J. Am. Chem. Soc.* **1991**, *113*, 944−949.
(30) Wan, Y.; Verkade, J. G. *J. Am. Chem. Soc.* **1995**, *117*, 141−156.
(31) Jurkschat, K.; Mugge, C.; Schmidt, J.; Tzschach, A. *J. Organomet. Chem.* **1985**, *287*, C1-C4.
(32) Jurkschat, K.; Tzschach, A.; Meunier-Piret, J.; van Meerssche, M. *J. Organomet. Chem.* **1986**, *317*, 145−151.
(33) Tzschach, A.; Jurkschat, K. *Pure Appl. Chem.* **1986**, *58*, 639−646.
(34) Mugge, C.; Pepermans, H.; Gielen. M.; Willem, R.; Tzschach, A.; Jurkschat, K. *Z. Anorg. Allg. Chem.* **1988**, *567*, 122−130.
(35) Boer, F. P.; Turley, J. W. *J. Am. Chem. Soc.* **1969**, *91*, 4134−4139.
(36) Kemma, A. A.; Bleidelis, J. J.; Zelchan, G. I. Urtrana, I. P.; Lukevits, E. J. *J. Struct. Chem. (English Translation)* **1977**, *18*, 268−271.
(37) Sidorkin, V. F.; Pestunovich, V. A.; Shagun, V. A.; Voronkov, M. G. *Doklady Chem. (English Translation)* **1977**, *233*, 160−163, and references therein.
(38) Hencsei, P.; Csonka, G. *Acta Chim. Acad. Sci. Hung.* **1981**, *106*, 285−290.
(39) Grabovskaya, Zh. E.; Klimenko, N. M.; Kartsev, G. N. *J. Struct. Chem. (English Translation)* **1987**, *28*, 840−845.
(40) Sidorkin, V. F.; Balakhchi, G. K.; Voronkov, M. G.; Pestunovich, V. A. *Doklady Chem. (English Translation)* **1987**, *296*, 400−403.
(41) Kartsev, G. N.; Klimenko, N. M.; Grabovskaya, Zh. E.; Chaban, G. M. *J. Struct. Chem. (English Translation)* **1988**, *29*, 931−933.
(42) Greenberg, A.; Plant, C.; Venanzi, C. A. *J. Mol. Struct. (THEOCHEM)* **1991**, *234*, 291−301.
(43) Gordon, M. S.; Carroll, M. T.; Jensen, J. H.; Davis, L. P.; Burggraf, L. W.; Guidry, R. M. *Organometallics* **1991**, *10*, 2657−2660.
(44) (a) Csonka, G. I.; Hencsei, P. *J. Organomet. Chem.* **1993**, *446*, 99−106. (b) Csonka, G. I.; Hencsei, P. *J. Mol. Struct. (THEOCHEM)* **1993**, *283*, 251. (c) Csonka, G. I.; Hencsei, P. *J. Organomet. Chem.* **1993**, *454*, 15−23.
(45) Csonka, G. I.; Hencsei, P. *J. Comput. Chem.* **1994**, *15*, 385−394.
(46) Gordon, M. S.; Davis, L. P.; Burggraf, L. W. *Chem. Phys. Lett.* **1989**, *163*, 371−374.
(47) Damrauer, R.; Burggraf, L. W.; Davis, L. P.; Gordon, M. S. *J. Am. Chem. Soc.* **1988**, *110*, 6601−6606.
(48) Windus, T. L.; Schmidt, M. W.; Gordon, M. S. *J. Am. Chem. Soc.* **1994**, *116*, 11449−11455.

Methods

The *ab initio* geometry optimizations performed here are quite time consuming, and in fact as noted above are made possible only because of the advent of parallel computers. All calculations were performed using the GAMESS electronic structure code, whose parallel SCF implementation has recently been described.[49] Preliminary AM1 or PM3 semiempirical calculations were performed using a version of MOPAC6[50] which has been incorporated into the GAMESS code. A typical run for the silatranes described herein utilized 128 nodes, 16 MBytes of memory per node, and was run in direct mode since the machines used have very limited I/O bandwidth. In most cases the semiempirical structure as well as Hessian matrix were used to begin an *ab initio* run, which then converged in about 25 geometry steps and about 400−800 min of machine time. A second important innovation which occured late in the project was the implementation of Pulay's group coordinates,[51] which particularly for the C_1 cases afford a great reduction in the number of steps required to find an optimal geometry.

The silatrane results are all obtained at the closed shell SCF (RHF) level,[52] and the majority of the calculations were made using the 6-31G(d) basis set.[53] A larger basis set, which will be referred to as EXT in this paper, was used to probe the effect of the basis set on the structures. The EXT basis extends the 6-31G(d) basis by using two sets of d functions[54a] on Si and its five adjacent heavy atoms as well as a diffuse sp shell[54b,c] situated on the same atoms. A few MP2 calculations[55] were performed to investigate the possible effect of electron correlation on the potential surfaces. The solution phase structures are modeled by the SCRF method.[56] Bonding analysis is carried out by orbital localization using the Boys algorithm.[57]

Structures are assumed to possess C_3 symmetry, or C_1 if the R group has lower symmetry. In the case of hydroxysilatrane, chlorocarbasilatrane, and both isomers of $CH_3Si[N(CH_3)CH_2CH_2]_3N$, we have successfully tested this assumption by computation of the analytic hessian by a parallel algorithm.[58] In addition, it is known that the silatranes possess C_3 or near-C_3 symmetry in the X-ray structures.

Structural Results

Gas Phase Geometries. The most important structural parameter of any silicon atrane is the SiN distance. These RHF/6-31G(d) bond lengths are gathered in Table 1, together with the available experimental data. A previous computation[45] has shown the C_3 system fluorosilatrane to be a minimum on the potential energy surface. We have computed the hessian for the C_1 case hydroxysilatrane and find that it too is a minimum energy structure.

Table 1. RHF/6-31G(d) Transannular (SiN) Bond Distances in the Silatranes $RSi[-Y(CH_2)_2-]_3N$[a]

R	Y = CH_2	Y = NH	Y = NCH_3	Y = O
H	2.636	2.311 (2.080)[b]	2.193	2.647 (2.146)
F	2.499	2.208	2.127 (2.034)[c]	2.534 (2.042, 2.324 ± 0.014)
OH	2.596 (2.477)[d]	2.287	2.181 (2.135)[e]	2.667 (2.11)[f]
NH_2	2.664	2.363		2.749
CH_3	2.691	2.385 (2.132)[g]	2.261	2.734 (2.175, 2.45 ± 0.05)
Cl	2.445	2.175	2.092	2.551 (2.023)
SH	2.547	2.227		2.627
PH_2	2.627	2.299		2.673
SiH_3	2.676	2.336		2.702

[a] All distances in Å. The first number in parentheses is the experimental X-ray value; the second is from gas phase electron diffraction, taken from ref 8 or 9, unless otherwise noted. [b] Reference 28. [c] Reference 30. [d] Reference 32. The compound is a bis ether, not OH. [e] Reference 23. The compound is OEt, not OH. [f] Reference 15. The compound is OMe, not OH. [g] Reference 22. The compound is C_6H_5, not CH_3.

It is well-known[8,9] that for silatranes the SiN bond distance is much shorter in the solid state than in the gas phase. However, the calculated structures in Table 1, which should reproduce gas phase experiments, have much longer SiN bond distances than the two available gas phase structures, for R = F and R=CH_3. The chief reason for the 0.28 Å change in SiN bond distance between the solid and gas state as well as the error in the computed structures, is the malleability of the silicon atranes. The central bond is actually not very strong, and thus rather large changes in this bond require very little energy.

This softness of the SiN bond is demonstrated in Figure 1. Part a of this figure shows an enlargement of the low energy portion of these potential curves. When the SiN bond distance is varied over a range of 0.5 Å on either side of the equilibrium position, the energy of the R = F carbasilatrane and azasilatrane varies by only 6−8 kcal/mol. Fluorosilatrane is even more deformable, requiring just 4 kcal/mol for the same range of SiN distortion. Clearly, crystal packing forces need not be larger than 1 kcal/mol to produce the observed 0.28 Å bond compression in silatranes.

Part b of Figure 1 shows the entire potentials, which we have extended to 1.5 Å past the equilibrium. Data similar to Figure 1 have been presented before for Y = O, at the semiempirical level[40,44] or using *ab initio* wave functions at semiempirical geometries.[43] Some of the semiempirical PM3 work[44] indicates there is a second minimum energy structure, denoted as the *exo* form, in which the nitrogen atom is inverted so that its lone pair is not directed at the Si. This occurs at around r(SiN) = 3.0 for the case of Y = O and R = F.[44a] It is clear from Figure 1 that there is no evidence of such a minimum on the Y = O, R = F *ab initio* potential, and thus the *exo* silatranes[44] are an artifact of the PM3 parameterization. Figure 1 also shows no sign of bond stretch isomerization for fluorocarbasilatrane, although initial NMR experiments[33] indicated this occurs for chlorocarbasilatrane. Later experiments[34] cast doubt on this interpretation, and in fact an explicit search by us for a long bond isomer of R = Cl, Y = CH_2 failed to find such an isomer. We have computed the analytic Hessian for the single, short bond isomer of chlorocarbasilatrane and found that it is a minimum on the potential energy surface. Finally, the most

(49) Schmidt, M. W.; Baldridge, K. K.; Boatz, J. A.; Elbert, S. T.; Gordon, M. S.; Jensen, J. H.; Koseki, S.; Matsunaga, N.; Nguyen, K. A.; Su, S.; Windus, T. L.; Dupuis, M.; Montgomery, J. A. *J. Comput. Chem.* **1993**, *14*, 1347−1363.

(50) Stewart, J. P. *J. Computer-Aided Mol. Design* **1990**, *4*, 1−105.

(51) (a) Pulay, P.; Fogarasi, G.; Pang, F.; Boggs, J. E. *J. Am. Chem. Soc.* **1979**, *101*, 2550−2560. (b) Fogarasi, G.; Zhou, X.; Taylor, P. W.; Pulay, P. *J. Am. Chem. Soc.* **1992**, *114*, 8191−8201.

(52) Roothan, C. C. J. *Rev. Mod. Phys.* **1951**, *23*, 69−89.

(53) (a) Hariharan, P. C.; Pople, J. A. *Theor. Chim. Acta* **1973**, *28*, 213−222. (b) Gordon, M. S. *Chem. Phys. Lett.* **1980**, *76*, 163−168. (c) Francl, M. M.; Pietro, W. J.; Hehre, W. J.; Binkley, J. S.; Gordon, M. S.; DeFrees, D. J.; Pople, J. A. *J. Chem. Phys.* **1982**, *77*, 3654−3665.

(54) (a) Each standard d exponent, e.g., ζ = 0.395 for Si (ref 53b), was multiplied by 0.4 and 1.4 to generate the 2d sets. (b) Clark, T.; Chandrasekhar, J.; Spitznagel, G. W.; Schleyer, P. *J. Comput. Chem.* **1983**, *4*, 294−301. (c) See footnote 13 of Frisch, M. J.; Pople J. A.; Binkley, J. S. *J. Chem. Phys.* **1984**, *80*, 3265−3269.

(55) Pople, J. A.; Binkley, J. S., Seeger, R. *Int. J. Quantum Chem.* **1976**, *S10*, 1−19.

(56) (a) Kirkwood, J. G. *J. Chem. Phys.* **1934**, 2, 351. (b) Onsager, L. *J. Am. Chem. Soc.* **1936**, *58*, 1486. (c) Szafan, M.; Karelson, M. M.; Katritzky, A. R.; Koput, J.; Zerner. M. C. *J. Comput. Chem.* **1993**, *14*, 371−377, and references therein.

(57) Boys, S. F. In *Quantum Science of Atoms, Molecules, and* Solids; Lowdin, P.-O., Ed.; Academic Press: New York, 1966.

(58) Windus, T. L.; Schmidt, M. W.; Gordon, M. S. *Chem. Phys. Lett.* **1993**, *216*, 375−379, using a parallel integral transformation described in Windus, T. L.; Schmidt, M. W.; Gordon, M. S. *Theor. Chim. Acta*, **1994**, *89*, 77−88.

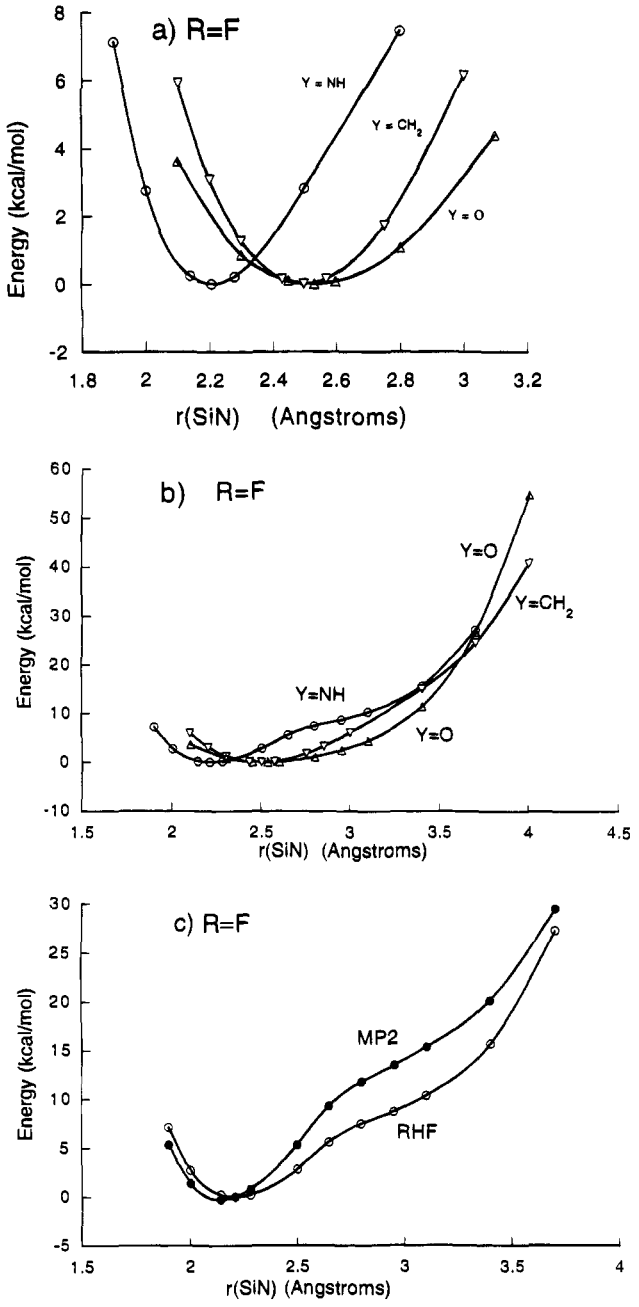

Figure 1. a) Low energy region of the fluorosilatrane potentials. b) The full potentials. c) Comparison of fluoroazasilatrane MP2 and SCF potentials.

interesting feature of Figure 1b is the wrinkle in the Y = NH potential near r(SiN) = 2.8 Å. In certain circumstances it is possible to find a minimum energy structure for other azasilatrane isomers near this value, as will be discussed below. This shoulder is not an artifact of the RHF method, as the same feature is evident in the MP2 potential (computed at the RHF geometries), as shown in Figure 1c.

Error Sources. Figure 1 also suggests the reason for the discrepancy between the computed and observed gas phase structures. Small errors due to basis sets or to the neglect of electron correlation could produce an apparently large change of geometry, at very little energy cost. We test these two possibilities separately.

We have examined the effect of the basis set by carrying out RHF/EXT geometry optimizations on the same three molecules shown in Figure 1. Both the change in the length of the SiN bond and the amount of energy lowering caused by reoptimization are of interest. The results are presented in the top half of Table 2. Fluoroazasilatrane's SiN bond decreases 0.025 Å and the energy lowers 0.2 kcal/mol upon optimization. Fluorocarbasilatrane is likewise little changed: the SiN bond decreases 0.028 Å and the energy decreases 0.1 kcal/mol. However, fluorosilatrane's SiN bond decreases significantly, by 0.117 Å, while gaining just a bit more energy during the reoptimization, 0.4 kcal/mol. The computed value of the SiN bond distance is 2.416 Å at the RHF/EXT level, removing just over half of the RHF/6-31G(d) discrepancy from the experimental value, 2.324 ± 0.014 Å.[18] The Y = O curve in Figure 1 is the only one whose minimum shifts significantly upon expansion of the basis set, so the Y = O curve should appear intermediate to the Y = NH and Y = CH_2 curves, rather than being almost coincident with the latter with the 6-31G(d) basis set.

Since the EXT basis set's diffuse functions and double d's had such a large effect on the silatrane geometry, we wondered about the possible effect of additional basis improvements. Adding a set of f functions (using literature exponents[54c]) to silicon and all adjacent atoms to produce an EXT+f basis once again caused an apparently large change in geometry. For fluorosilatrane, the transannular distance increases by 0.08 to 2.49 Å, canceling most of the shortening obtained by expansion to the EXT basis. Once again, the energy influence is small, as reoptimization with the f's lowers the energy by only 0.17 kcal/mol. It is clear that the EXT+f results presented here are unlikely to be converged with respect to the basis set.

Of course, it is also possible that a correlated calculation such as MP2 is needed to remove the remaining error. The MP2 curve presented in Figure 1c suggests such a possibility, as single point MP2 energies along the SCF potential curves have their minima apparently shifted inwards. For R = F, the decrease in SiN bond distance at the MP2 level for Y = O, NH, and CH_2 is 0.24, 0.06, and 0.15 Å, respectively. These numerical results should be viewed with some caution, as they do not include full geometry optimization at the MP2 level, and they are obtained with the 6-31G(d) basis. Nonetheless, they indicate that the Y = O atranes, which have the softest stretching potentials, also have the largest change in geometry beyond the SCF level.

Based on the discussion in the preceding three paragraphs, and the two available Y = O gas phase structures, it seems likely that the RHF/6-31G(d) structures reported in Table 1 contain a systematic error in r(SiN) for Y = O of about 0.22–0.28 Å. The error for Y = CH_2 and Y = NH (and presumably Y = NCH_3) is likely to be smaller, with the results in Table 1 being perhaps 0.05–0.15 Å too long, with the azasilatrane error lying near the lower end of this range. It is also clear that a quantitative calculation of the geometry of a Y = O silatrane would be very demanding, as both large basis sets and electron correlation are necessary.

Solution Geometries. Even after taking account of these error estimates in the computed gas phase structures, there still remain large discrepancies between the computed and X-ray values in Table 1. These must be due to the change of medium from the (computed) gaseous state to the solid. While we cannot perform any computation which would mimic the solid state, recall that silatranes are thought to have intermediate SiN bond lengths in solution.[19] It is possible to qualitatively investigate the effect of solvation upon the molecular geometry using the Onsager reaction field cavity model.[56] The geometries were reoptimized using this simplistic solution model for R = F and Y = CH_2, NH, or O, using the EXT basis set. Each molecule was placed in a cavity of radius a_0 = 3.67 Å, derived from the

Table 2. Basis Set and Medium Effects on R = F Atranes

	Y = CH_2	Y = NH	Y = O	
	gas, RHF/6-31G(d)			
r(SiN)	2.499	2.208	2.534	Å
r(SiF)	1.640	1.630	1.587	Å
	gas, RHF/EXT			
r(SiN)	2.471	2.183	2.416	Å
r(SiF)	1.641	1.635	1.587	Å
E(optimization)	0.07	0.22	0.44	kcal/mol
dipole	4.3	5.0	7.5	Debye
	DMSO, RHF/EXT			
r(SiN)	2.332	2.100	2.104	Å
r(SiF)	1.678	1.667	1.638	Å
E(solvation)	3.82	5.02	10.55	kcal/mol
E(optimization)	0.68	0.82	4.12	kcal/mol
dipole	7.5	8.2	13.0	Debye

experimental density of 1.552 g/cm^3 for fluorosilatrane,[59] using a dielectric constant of $\epsilon = 45$ to simulate DMSO.

The striking results of reoptimization in DMSO "solution" are included in Table 2. Each of the three atranes undergoes a dramatic shortening of the SiN bond length, 0.14 for Y = CH_2, 0.08 for Y = NH, and 0.31 Å for Y = O! The amount of energy gained by reoptimizing the geometry is less than 1 kcal/mol for the first two molecules but is 4 kcal/mol for fluorosilatrane. The solution phase SiN bonds in Y = NH and Y = O are essentially equal and in fact approach the solid state X-ray distances given in Table 1.

A physical interpretation of the large change in geometry hinges on two factors, namely the softness of the SiN bond already noted in Figure 1 and the large dipole moments of these compounds (Table 2). To understand the role played by the latter it is necessary to digress into the specifics of the Onsager model.[56] This model represents the interaction energy of a neutral solute in a spherical cavity embedded in a continuum dielectric by permitting the dipole of the solute to induce a dipole within the dielectric. The induced dipole in turn influences the dipole of the solute, so these dipoles are iterated to self-consistency. The energy of the interaction ("solvation energy") is

$$E_{solv} = -{}^1/_2\mathbf{R}\cdot\mu$$

where the induced dipole **R** depends on the dielectic of the solvent (ϵ), the radius of the cavity containing the solute (a_0), and the solute dipole (μ):

$$\mathbf{R} = g\mu, \quad g = 2(\epsilon - 1)/(2\epsilon + 1)a_0 3$$

For a given cavity size and dielectric constant, as in the present calculations, the interaction energy will be larger for solutes with larger dipoles. Thus, the energy lowering due to solvation at the gas phase geometry as well as the energy lowering produced by geometry reoptimization in the solvent field increases in the order Y = CH_2 < NH < O. As was already noted in the pioneering semiempirical study of solution effects on silatrane geometry,[40] the dipole moment increases when the SiN bond decreases under the influence of solvent. Increasing the solute dipole increases the solvent interaction, in turn providing additional driving force to further decrease the SiN bond. However, the large dipoles reported in Table 2 are able to generate the large changes in the SiN distance only because this bond is easily compressed at little energy cost.

(59) Parkanyi, L.; Hencsei, P.; Bihatsi, L.; Muller, T. *J. Organomet. Chem.* **1984**, *269*, 1–9.

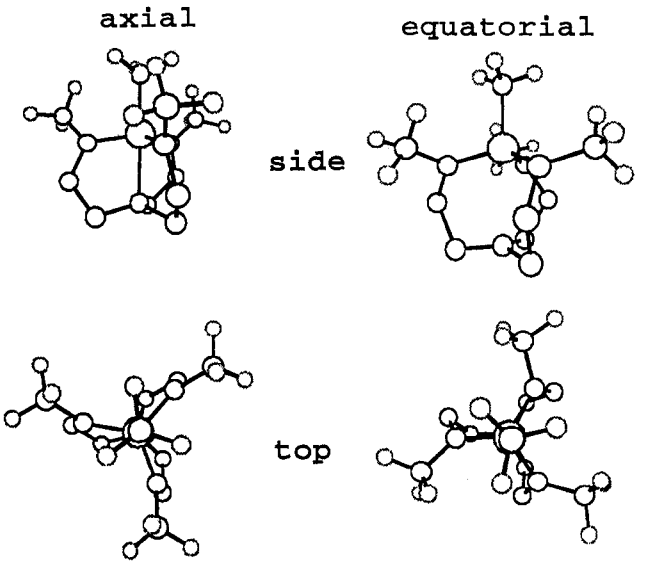

Figure 2. Side and top views of the axial and equatorial isomers of the R = CH_3, Y = NCH_3 azasilatrane. The hydrogens on the side chains have been omitted for clarity. The sum of the bond angles around the equatorial N atoms is 356.1 and 358.0 degrees in the axial and equatorial isomers.

Table 3. RHF/6-31G(d) Azasilatrane Axial and Equatorial Isomers[a]

		r(SiN$_{ax}$)		r(SiN$_{eq}$)		
R	Y	ax	eq	ax	eq	ΔE
H	NH	2.310		1.751		
CH_3	NH	2.385	2.751	1.755	1.740	+3.2
H	NCH_3	2.193	2.722	1.767	1.738	+6.1
CH_3	NCH_3	2.261	2.896	1.780	1.742	−2.4

[a] Distances are in Å, and the energy difference E(eq) − E(ax) is in kcal/mol.

Azasilatrane Isomerization. The substituent on an equatorial N has an interesting affect on the molecular geometry, which is not possible with either Y = O or Y = CH_2. The equatorial nitrogens have both a functional group and a lone pair, and interchanging these two yields distinct isomers. The possible positions occupied by the functional group X are "axial" such that the NX bond is approximately parallel to SiR or "equatorial" with the X group lying approximately in the plane of the three nitrogens. Figure 2 illustrates what we mean by an "axial" or "equatorial" X group. The data shown in Table 1 in all cases correspond to the axial isomer.

We have explored the affect of instead placing the X groups equatorial for R = H and CH_3, with Y = NH and Y = NCH_3. The results are shown in Table 3. With small groups R = H and Y = NH, it is impossible to locate an equatorial isomer, as all trial structures revert to the axial geometry after optimization. However, for the other three cases both C_3 local minima are found to exist. For the case R = X = CH_3, we have verified that both isomers are indeed relative minima on the potential surface by computation of the Hessian matrices, which have all real frequencies. Placing the X group in the equatorial orientation has a large effect on the transannular bond distances, which increase 0.36–0.59 Å. There is a smaller change in r(SiN$_{eq}$) in the opposite direction. When the smaller group H is present at either R or X, the equatorial isomer is energetically slightly less stable. However, when the slightly bulkier methyl group is used for both R and X, the equatorial isomer is more stable by a small amount, 2 kcal/mol. These equatorial isomers all occur near r(SiN) = 2.8, where Figure 1b exhibits a shoulder for the case R = F, Y = NH. We regard the possible steric

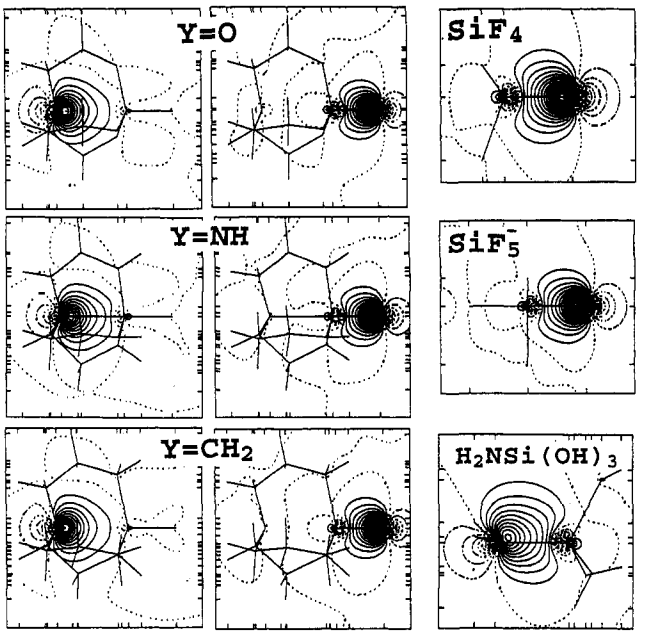

Figure 3. RHF/EXT Boys localized orbitals for the R = F silicon atranes, compared to other SiF and SiN bonds. In these plots, N is at the left, Si to the right, and F at the extreme right.

crowding of the R and X groups as the cause of the existence of two isomers, which consequently have two different transannular SiN bond distances.

The existence of this kind of bond-stretch isomerization is supported by the two published X-ray structures which have located the substituent on the equatorial N. For R = OEt and Y = NCH_3, the methyl groups take an axial orientation,[23] with r(SiN) = 2.135 Å. However, with R = CH_3, use of the very bulky Y = $NSi(CH_3)_3$ forces an equatorial orientation,[24] and r(SiN) = 2.775 Å. Our computed structures for both R = CH_3 and Y = NCH_3 isomers are shown in Figure 2. The equatorial isomer is clearly less sterically hindered around Si. A more subtle change in the geometry is an increased ring pucker at the methylene atom adjacent to the equatorial nitrogen, opposite to the direction of this nitrogen's substituent. This same puckering, like the flap of an envelope ring conformation, is also evident in the published ORTEP structure[24] and must be the cause of sufficient ring strain to open the weak SiN transannular bond. Note that the base nitrogen in the equatorial isomer in Figure 2 is nearly flat, but its small degree of pyramidalization is still directed toward Si, as is true experimentally.[24]

It is interesting to note from Table 1 that replacing Y = NH by Y = NCH_3 produces a decrease in the SiN bond length. The decrease is about 0.08 Å but is somewhat larger for R = H. Unfortunately there is no experimental light to be shed on this methyl affect, since the available X-ray structures do not include the same R for both Y = NH and Y = NCH_3.

Localized Orbitals and Bonding

Before discussing the extent of SiN bonding in the silicon atranes, it is appropriate to review prior thinking about this bond. Not surprisingly, the first bonding model[2] for atranes in the 1960s invoked the then popular sp^3d model for trigonal bipyramidal geometries. The three center, four electron bonding model of Musher[60] caused a re-valuation of this bond in those terms by 1977.[61] Recently, five coordinate silicon compounds with SiN bonds similar to the atranes have been described as being primarily dative in character.[62] Thus, the bonding models have progressed steadily toward weaker descriptions.

The Boys localized orbitals[57] of the three R = F silicon atranes are shown in Figure 3. For comparison, the normal covalent SiN and SiF bonds in silanes are shown, along with the hypervalent axial bond in SiF_5^-. The normal valent and hypervalent SiF bonds have essentially identical contour plots, and so it is not possible to characterize the SiF bonds in the atranes as one or the other. However, the SiN bonds in the atranes have a very different shape than the normal covalent SiN bond in $H_2N-Si(OH)_3$. It is clear that the atrane SiN "bonds" are best described as nitrogen lone pairs, interacting only slightly with the silicon atoms.

The localized orbitals clearly support the dative bonding model of Haaland.[62] Additional features of this model include the prediction of large changes in bond distance with inductive effects at the acceptor atom, weak donor–acceptor bond strengths, and a preference for the donor to occupy axial postions. All of these are certainly true of the silicon atranes.

It should be pointed out that the three center, four electron (3c4e) model and the dative bonding model represent limiting extremes of the same basic MO diagram:

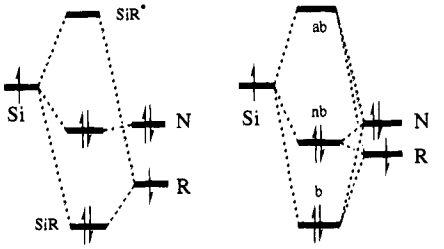

On the left, the primary interaction is the formation of a bond and antibond between SiR, with the nitrogen lone pair remaining essentially unaffected during molecular formation. The only SiN binding is provided by a small dative interaction. On the right, all three orbitals contribute to the formation of the 3c4e bonding (b), nonbonding (nb), and antibonding (ab) levels. Note that instead of the usual donation of two electrons by the center atom, in this case the electron pair comes from the nitrogen ligand. Since the two diagrams differ only in the degree of interaction, they can be distinguished only by detailed quantum mechanical computation of the LCAO molecular orbital coefficients.

As was already shown by the contour plots in Figure 3, the SiN bond is well described using the dative MO diagram on the left. This diagram predicts an ordinary covalent SiR bond, whereas the 3c4e diagram on the right would predict an elongated SiR bond.

The computed SiR bond distances are shown in Table 4, which also includes the covalent SiR bond distances in the analogous silanes. The covalent bond distances increase by 0.02–0.04 Å from $RSi(OH)_3$ to $RSi(CH_3)_3$. Three of the atranes (Y = O, R = H, F, Cl) possess shorter SiR bonds than in the corresponding silanes. Note however from Table 2 that shortening the SiN bond in solution leads to a SiF bond in fluorosilatrane that is longer than in the corresponding silane. For the remaining atranes the SiR bond is longer than in the corresponding silane, by 0.01–0.08 Å. The two largest elongations occur for R = Cl, Y = CH_2 or NH. The elongations are somewhat smaller than the 0.10 Å increase in the SiF bond distance in going from SiF_4 (RHF/EXT bond distance 1.556 Å) to SiF_5^- (equatorial 1.618, axial 1.658 Å). The small but

(60) Musher, J. I. *Angew. Chem., Int. Ed. Engl.* **1969**, *8*, 54–59.
(61) Sidorkin, V. F.; Pestunovich, V. A.; Voronkov, M. G. *Doklady Phys. Chem. (English Translation)* **1977**, *235*, 850–853.
(62) Haaland, A. *Angew. Chem., Int. Ed. Engl.* **1989**, *28*, 992–1007.

Table 4. RHF/6-31G(d) Substituent (Si−R) Bond Distances in the Silatranes and the Model Silanes $RSi(YH)_3$

	Y = CH_2		Y = NH		Y = O	
R	silatrane	silane	silatrane	silane	silatrane	silane
H	1.503	1.489	1.500	1.484	1.465	1.468
F	1.640	1.615	1.620	1.603	1.587	1.592
OH	1.689	1.654	1.682	1.654	1.634	1.633
NH_2	1.764	1.742	1.759	1.725	1.707	1.703
CH_3	1.912	1.896	1.906	1.885	1.862	1.858
Cl	2.171	2.100	2.167	2.091	2.063	2.071
SH	2.224	2.177	2.227	2.164	2.141	2.134
PH_2	2.314	2.283	2.318	2.271	2.250	2.247
SiH_3	2.392	2.371	2.401	2.363	2.344	2.343

noticeable increase in SiR distances suggests that the bonding is somewhere between the idealized dative and 3c4e MO diagrams drawn above, while the contour plots suggest this intermediate position is closer to the dative picture.

In order to achieve good 3c4e bonding, electronegative axial groups and an electropositive central atom are needed.[60] Thus, we observe from Table 1 a steady shortening of the SiN bond from R = CH_3 to R = F and again from R = SiH_3 to R = Cl. From the 3c4e MO diagram shown above, we note that there will be better orbital mixing when the energy of the R orbital is closer to that of the nitrogen lone pair. Thus, for third period R compared to the analogous second period R, Table 1 shows r(SiN) is consistently smaller, while Table 4 shows r(SiR) is consistently more elongated. Both trends indicate a larger extent of three center bonding with third period substituents. In fact, R = Cl produces the shortest SiN bonds. An earlier study of neutral five coordinate silicon compounds by our group[46] also found that Cl is an ideal axial partner for ammonia. In the current work, the computed gas phase structure with the shortest SiN bond is that with R = Cl, Y = NCH_3. It is quite possible that the solid state structure of this azasilatrane will be found to have a SiN bond distance shorter than 2 Å, making it the shortest known.

Summary

The geometry of the silicon atranes has been found to vary considerably as a function of a wide range of substituents R but is actually affected more by the choice of the equatorial group Y. Azasilatranes possess the shortest SiN distances, followed by silatranes, and then carbasilatranes. The SiN bond is a weak one, requiring no more than 8 kcal/mol to stretch it over a 1 Å range. This flexibility, coupled with the large dipole moments of the atranes, causes large changes in their geometry upon change of state from gas to condensed media, as demonstrated by approximate solvent calculations. Bond-stretch isomerization is predicted to occur in the azasilatranes, depending on the bulk of the ligands at silicon and the equatorial nitrogens. Chlorine atoms are the most effective axial partner for the basal nitrogen, and the azasilatrane R = Cl, Y = NCH_3 is predicted to have a shorter SiN bond distance than for any currently measured silicon atrane. Bonding in the silicon atranes is best described as a dative N → Si bond but with sufficient three center interaction to produce a slight elongation of the SiR bond.

Acknowledgment. The authors would like to thank Jan Jensen for advice on what the SCRF solvent model can and cannot do and for assistance with the group coordinates. Discussions with Professor Verkade throughout the project have been most helpful as well. The great majority of the computations were performed on the Touchstone Delta parallel computer, under the auspices of an ARPA sponsored program with the Air Force Phillips Lab, with some additional calculations performed on the CM-5 located at the Army High Performance Computer Center. Solvent computations were performed on the Paragon located at San Diego Supercomputing Research Center. The MP2 single point computations were performed on an IBM SP2, purchased under the NSF equipment grant CHE93-19163, and using a parallel MP2 algorithm written by Michel Dupuis. The analytic Hessians were computed on a SGI Power Challenge belonging to Ames Laboratory's Scalable Computing Group. The research presented here was supported from the Air Force Office of Scientific Research (93-0105) and the National Science Foundation (CHE94-11911).

JA941869I